

The density matrix renormalization group applied to single-particle quantum mechanics

This article has been downloaded from IOPscience. Please scroll down to see the full text article.

1999 J. Phys. A: Math. Gen. 32 6079

(<http://iopscience.iop.org/0305-4470/32/33/306>)

View [the table of contents for this issue](#), or go to the [journal homepage](#) for more

Download details:

IP Address: 171.66.16.105

The article was downloaded on 02/06/2010 at 07:39

Please note that [terms and conditions apply](#).

The density matrix renormalization group applied to single-particle quantum mechanics

M A Martín-Delgado[†], G Sierra[‡] and R M Noack[§]

[†] Departamento de Física Teórica I, Universidad Complutense, Madrid, Spain

[‡] Instituto de Matemáticas y Física Fundamental, CSIC, Madrid, Spain

[§] Institut de Physique Théorique, Université de Fribourg, CH-1700 Fribourg, Switzerland

Received 12 March 1999

Abstract. A simplified version of White's density matrix renormalization group (DMRG) algorithm has been used to find the ground state of the free particle on a tight-binding lattice. We generalize this algorithm to treat the tight-binding particle in an arbitrary potential and to find excited states. We thereby solve a discretized version of the single-particle Schrödinger equation, which we can then take to the continuum limit. This allows us to obtain very accurate results for the lowest energy levels of the quantum harmonic oscillator, anharmonic oscillator and double-well potential. We compare the DMRG results thus obtained with those achieved by other methods.

1. Introduction

The density matrix renormalization group (DMRG) method [1] originated from the study of a very simple problem: the quantum behaviour of a single particle on a lattice [2]. The standard renormalization group (RG) method applied to this problem fails completely and the understanding of this failure was the key that led to the DMRG. The DMRG has since been successfully applied to interacting many-body problems in condensed matter and statistical mechanics and it is very promising in atomic, molecular and nuclear physics and field theory (see [3, 4] for an overall account of the DMRG). In view of all these developments, it is interesting to come back to the origin of the DMRG and see how it works for a single particle under the action of a potential. This problem is not purely academic since it provides a testbed for new ideas and techniques relating to the DMRG in simple models provided by quantum mechanics (QM). In addition, these simple models can contain interesting physics. For example, the instantons of gauge theories have a very nice analogue in the double-well potential. We also hope that the DMRG will provide an accurate new method to solve the Schrödinger equation numerically.

2. The problem

The purpose of this paper is to present a DMRG algorithm for finding the ground state and excited states of a particle confined to the real line $-\infty < x < \infty$, and whose dynamics is governed by the Hamiltonian $H = p^2 + V(x)$, where p^2 is the kinetic energy and $V(x)$ is the potential energy. The first step before we can apply the DMRG to QM is to discretize the Schrödinger Hamiltonian H . This can be done by constraining the position of the particle to take on the discrete values $x_n = h(n - \frac{N+1}{2})$, ($n = 1, 2, \dots, N$), where N is the number

of allowed sites and h is the lattice spacing. The particle is thus confined to a box of size $R = x_N - x_1 = h(N - 1)$. After this discretization, the Hamiltonian $H = p^2 + V(x)$ becomes the $N \times N$ matrix

$$H_{n,m} = \begin{cases} 2/h^2 + V_n & n = m \\ -1/h^2 & |n - m| = 1 \\ 0 & \text{otherwise} \end{cases} \quad (1)$$

where $V_n = V(x_n)$. Conversely, one can recover the Schrödinger Hamiltonian from equation (1) by taking the continuum limit $h \rightarrow 0$, $N \rightarrow \infty$ with $R = N \times h$ kept fixed, and then letting $R \rightarrow \infty$. In the free case, $V(x) = 0$, the discrete Hamiltonian, equation (1), coincides, up to the overall factor $1/h^2$, with the Hamiltonian studied by White and Noack in [2].

3. The DMRG algorithm

The problem is to diagonalize the $N \times N$ matrix, equation (1), using DMRG methods. The basic strategy is to split the box of length N into a left block B_ℓ^L with ℓ sites, two middle sites $\bullet\bullet$ and a right block $B_{N-\ell-2}^R$ with $N - \ell - 2$ sites, so that the whole system can be represented as $B_\ell^L \bullet\bullet B_{N-\ell-2}^R$. If no truncation is performed, B_ℓ^L contains all the degrees of freedom associated with the ℓ sites on the left-hand side, and similarly $B_{N-\ell-2}^R$ describes all the degrees of freedom on the right-hand side.

The DMRG method is based on the idea that the low-energy properties of the system can be described by a few degrees of freedom. In particular, if we are only interested in the ground state of the system we may simply consider the blocks B_ℓ^L and $B_{N-\ell-2}^R$ to be described by a single degree of freedom. The effective Hamiltonian of the system then becomes a 4×4 matrix whose diagonalization is straightforward. Once this is done, the next step is to make a partition of the system either as $B_{\ell+1}^L \bullet\bullet B_{N-\ell-3}^R$ or as $B_{\ell-1}^L \bullet\bullet B_{N-\ell-1}^R$, i.e. make the left or right side grow by one site, and repeat the diagonalization. One then iterates this procedure, moving the position of the partition, ℓ , leftwards and rightwards through the lattice. After several such sweeps through the lattice, the DMRG converges to a fixed-point solution which reproduces the ground state of the free tight-binding particle to high accuracy.

3.1. Superblock Hamiltonian

This method can be generalized to treat the $N_E \geq 1$ lowest energy levels, i.e. $N_E - 1$ excited states. The basic idea is that the left and right blocks B^L and B^R must contain N_E degrees of freedom, one for each low-energy state. The superblock Hamiltonian H_{SB} is therefore a $(2N_E + 2) \times (2N_E + 2)$ matrix given by

$$H_{SB} = \begin{pmatrix} H_L & -v_L & 0 & 0 \\ -v_L^\dagger & h_{CL} & -1/h^2 & 0 \\ 0 & -1/h^2 & h_{CR} & -v_R^\dagger \\ 0 & 0 & -v_R & H_R \end{pmatrix} \quad (2)$$

where H_L and H_R are $N_E \times N_E$ matrices, v_L and v_R are N_E -component column vectors, and h_{CL} and h_{CR} are real numbers. The meaning of these quantities is as follows: H_L is the Hamiltonian which describes the interactions inside the block B^L , $-v_L$ describes the interaction between B^L and the site next to it in the superblock $B^L \bullet\bullet B^R$ and h_{CL} is the Hamiltonian on a single site. The quantities H_R , $-v_R$ and h_{CR} for the right half have an analogous meaning. The two terms proportional to $-1/h^2$ in equation (2) come directly from the off-diagonal terms in equation (1).

The Hamiltonian, equation (2), describes the superblock $B_\ell^L \bullet \bullet B_{N-\ell-2}^R$ and depends on the value of ℓ , i.e. $H_{SB} = H_{SB}^{(\ell)}$. In particular, the diagonal entries h_{CL} and h_{CR} are given by

$$h_{CL} = \frac{2}{h^2} + V_{\ell+1} \quad h_{CR} = \frac{2}{h^2} + V_{\ell+2}. \quad (3)$$

Since the blocks $B^{L,R}$ contain N_E effective sites, $H_{SB}^{(\ell)}$ can be defined for $\ell = N_E, N_E + 1, \dots, N - N_E - 2$.

3.2. DMRG truncation

The superblock can be used either to enlarge the left block by one site, i.e. $B_\ell^L \bullet \rightarrow B_{\ell+1}^L$, or the right block. Let us examine how to do this for the left block. For $N_E = 1$, the ground state of the superblock Hamiltonian, equation (2), has four components, which we designate $(a_L, a_{CL}, a_{CR}, a_R)$. The projection of this state onto $B^L \bullet$ yields (a_L, a_{CL}) , which must then be normalized by dividing by $N_a = \sqrt{a_L^2 + a_{CL}^2}$. The new effective Hamiltonian, H'_L , and v'_L are then given by

$$H'_L = (a'_L, a'_{CL}) \begin{pmatrix} H_L & -v_L \\ -v_L & h_{CL} \end{pmatrix} \begin{pmatrix} a'_L \\ a'_{CL} \end{pmatrix} \quad (N_E = 1) \quad (4)$$

and

$$v'_L = a'_{CL} \quad (5)$$

where $a'_L = a_L/N_a$ and $a'_{CL} = a_{CL}/N_a$.

We next describe how to generalize this construction to $N_E > 1$. First we have to obtain the lowest N_E eigenstates of H_{SB} , which we shall denote as $\{(a_{L,i}, a_{CL,i}, a_{CR,i}, a_{R,i})\}_{i=1}^{N_E}$, where $a_{L,i}$ and $a_{R,i}$ are N_E -component vectors. These vectors are projected onto a set of N_E vectors of the block $B^L \bullet$, i.e., $\{(a_{L,i}, a_{CL,i})\}_{i=1}^{N_E}$. Since this set of vectors is not generally orthogonal, we orthonormalize them explicitly. Let us call the set of vectors so obtained $\{(a'_{L,i}, a'_{CL,i})\}_{i=1}^{N_E}$. The projection $B^L \bullet \rightarrow B'^L$ is performed by an $(N_E + 1) \times N_E$ matrix

$$A' = \begin{pmatrix} a'_{L,1} & \dots & a'_{L,N_E} \\ a'_{CL,1} & \dots & a'_{CL,N_E} \end{pmatrix}. \quad (6)$$

Operators associated with B'^L are transformed into the new basis via

$$H'_L = A'^{\dagger} \begin{pmatrix} H_L & -v_L \\ -v_L & h_{CL} \end{pmatrix} A' \quad (7)$$

and

$$v'_{L,i} = a'_{CL,i} \quad (i = 1, \dots, N_E). \quad (8)$$

Observe that we do not need to construct a density matrix to define a unique projection. This is a peculiarity of the single-particle nature of the problem. In a many-body problem, we would have to perform the projection using the reduced density matrix due to the non-single-valuedness of the projected wavefunctions.

3.3. Initialization and sweeps

The finite-system DMRG algorithm consists of a warm-up phase in which the system is built up to its actual length N , followed by several leftwards and rightwards ‘finite-system’ sweeps which are repeated until convergence is achieved. The initial superblock of the warm-up phase

is taken to be $B_{N_E}^L \bullet \bullet B_{N_E}^R$, where H_L (H_R) are taken to be the first (last) N_E entries of the matrix, equation (1), i.e.

$$\begin{aligned} H_L &= (h_{n,m}, n, m = 1, \dots, N_E) \\ H_R &= (h_{n,m}, n, m = N - N_E + 1, \dots, N). \end{aligned} \quad (9)$$

Similarly, $v_L = (0, 0, \dots, 1)$ and $v_R = (1, 0, \dots, 0)$. For a symmetric potential, i.e. $V(-x) = V(x)$, the quantities H_R, v_R for the right side can be obtained from the left ones by the reflection operation, $n \rightarrow N_E - n + 1$. This property applies at each step of the warm-up phase of the algorithm and corresponds to the well known reflection operation of the infinite-system DMRG algorithm for interacting systems. Of course, for a non-symmetric potential the right block, B^R , cannot be formed by reflecting the left one, B^L .

The behaviour of the location of the added site, ℓ , during the warm-up process and the first sweep can be summarized in the following scheme:

$$\begin{aligned} \text{warm-up:} \quad \ell &= N_E, \dots, \frac{N}{2} - 1 \\ \text{left} \rightarrow \text{right:} \quad \ell &= \frac{N}{2}, \dots, N - N_E - 2 \\ \text{right} \rightarrow \text{left:} \quad \ell &= N - N_E - 2, \dots, N_E \\ \text{left} \rightarrow \text{right:} \quad \ell &= N_E, \dots, \frac{N}{2} - 1 \end{aligned} \quad (10)$$

where we take N to be even. We define a sweep to be a complete cycle that ends when the two sites of the superblock $B_\ell^L \bullet \bullet B_{N-\ell-2}^R$ are in the middle of the chain.

4. Analysis of errors

In this paper we present the results obtained with the DMRG algorithm applied to three well known potentials and compare them with the results of other methods. The three potentials we shall consider are the harmonic oscillator, the anharmonic oscillator and the double-well potential.

In order to take the continuum limit, we enlarge the number of lattice sites, N , while taking the discretization step, h , to be smaller and smaller so that $R = N \times h$. During this process, it is important to determine the accuracy of the DMRG results for the energy levels as N increases. To this end, we first compare the DMRG results with the known exact results for the tight-binding particle with fixed boundary conditions at the ends. The exact spectrum is given by:

$$\Psi_n(j) = N_n \sin \frac{\pi(n+1)}{N+1} j \quad E_n^{(ex)} = 4 \sin^2 \left(\frac{\pi(n+1)}{2(N+1)} \right) \quad (11)$$

where $n = 0, 1, \dots, N-1$ denotes the energy levels, $j = 1, 2, \dots, N$ are the lattice sites and the N_n are normalization constants.

We have made runs targeting the $N_E = 1, 2, 3$ lowest-lying states and have computed the relative error of the energy levels,

$$\delta E_i = |(E_i(DMRG) - E_i^{(ex)})/E_i^{(ex)}| \quad i = 1, \dots, N_E. \quad (12)$$

For $N_E = 1$, a slowing down of the convergence and, eventually, numerical instabilities due to round-off error appear on chains of length of order 500 or greater due to a vanishing matrix element connecting the blocks. Since this problem does not occur when $N_E \geq 2$, we take $N_E \geq 2$ in the following.

In figure 1, we plot the relative error in the ground state energy for $N_E = 2$ and 3 as a function of N . These results were obtained with the finite-system algorithm described

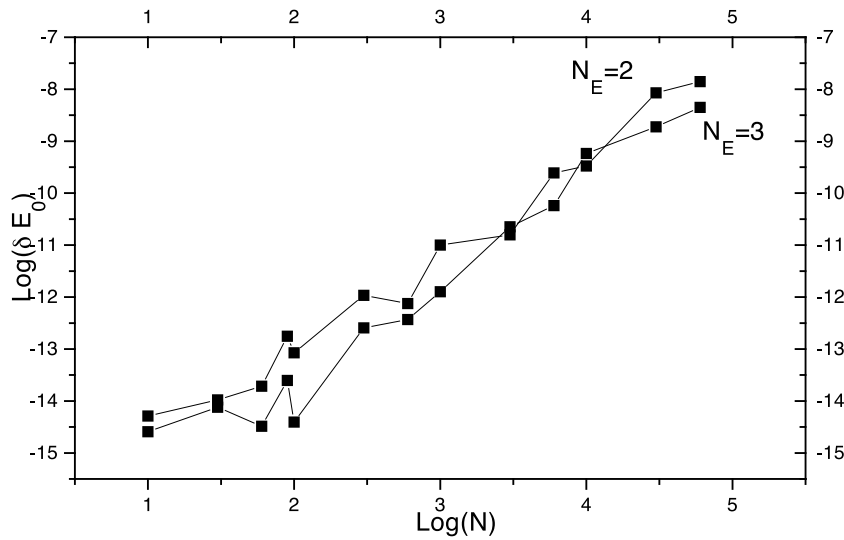


Figure 1. Logarithm of the relative error in the ground state energy of a free particle on a tight-binding lattice as a function of the logarithm of the number of sites of the chain, varying the number of targeted states, N_E .

above, taking a sufficient number of finite-system sweeps to obtain convergence. Typically, convergence was achieved after five sweeps. In this plot we see that for a fixed number of targeted states, N_E , the error increases with the number of sites N . The range goes from $\delta E_0 = 5.1 \times 10^{-15}$ for $N = 10$ to $\delta E_0 = 1.4 \times 10^{-10}$ for $N = 60\,000$ ($N_E = 2$), while $\delta E_0 = 2.6 \times 10^{-15}$ for $N = 10$ and $\delta E_0 = 4.4 \times 10^{-9}$ for $N = 60\,000$ ($N_E = 3$). Likewise, when the number N_E is increased we observe that the errors decrease and this effect is more apparent when the number of sites N is bigger. In figure 2, we plot analogous results for the first excited state, and find that the error behaves essentially the same as for the ground state.

The lesson to be learned from this analysis is that care must be taken when going to large lattice sizes because the DMRG tends to loose numerical accuracy with increasing N . On the other hand, targeting a larger number of states N_e actually *improves* the accuracy of each state. In going to the continuum limit, there is therefore a trade-off between the discretization error which can be reduced by taking N large, and the error in the DMRG results [5].

5. The harmonic oscillator

We first apply the continuum limit of the DMRG to a simple and exactly solvable model: the harmonic oscillator. We write the Hamiltonian

$$H = P^2 + X^2 \quad (13)$$

where $P = -i \frac{d}{dx}$. The corresponding exact spectrum with this normalization is $E_n = 2n + 1$, $n = 0, 1, \dots$. We can use this example to calibrate the accuracy of the DMRG by comparing with the exact solution. In table 1, we present the results for the two lowest eigenstates, for which $E_0 = 1$ and $E_1 = 3$. These results are obtained using five finite-system sweeps. We have checked that we obtain the same results to within roundoff error when performing up to 20 sweeps. We measure the DMRG energies during the final sweep in the configuration in which the left block and the right block are the same size, i.e. the single sites in the superblock

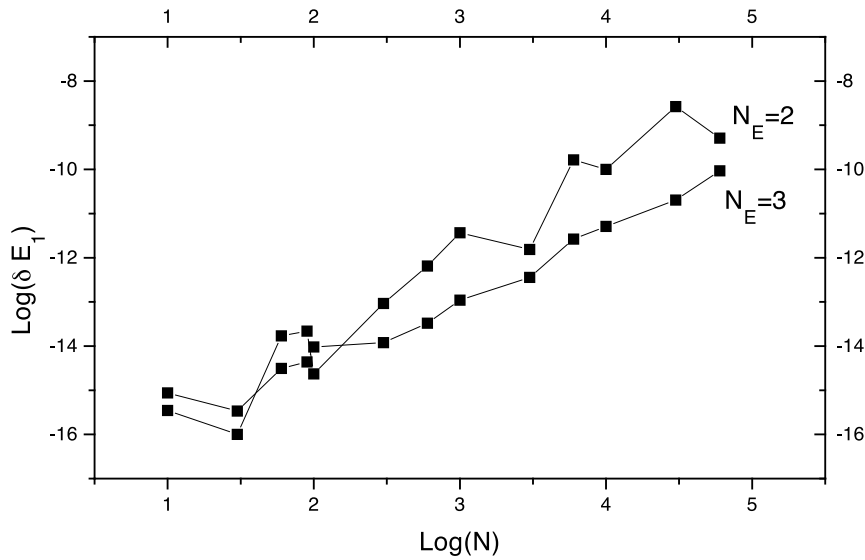


Figure 2. Logarithm of the relative error in the first excited state energy of a free particle on a tight-binding chain as a function of the logarithm of the number of sites of the chain, varying the number of targeted states, N_E .

Table 1. The difference between the exact continuum energies, $E_n = 2n + 1$, and the energies on the discretized lattice, $E_0(N)$ and $E_1(N)$, for the ground and first excited states of the harmonic oscillator obtained with the DMRG and exact diagonalization. Here N is the number of sites on the chain, h is the discretization step and R is the size of the continuum system. The errors (digits in parentheses) are determined using the GCC procedure explained in the text.

Method	N	h	$R = N \times h$	$1.0 - E_0(N)$	$3.0 - E_1(N)$
DMRG	100	0.1	10	$6.253\,912\,540(370) \times 10^{-4}$	$3.128\,521\,663(378) \times 10^{-3}$
Exact diag.	100	0.1	10	$6.253\,912\,540\,310 \times 10^{-4}$	$3.128\,521\,663\,376 \times 10^{-3}$
DMRG	1 000	0.01	10	$6.249\,89(322) \times 10^{-6}$	$3.124\,333\,8(564) \times 10^{-5}$
Exact diag.	1 000	0.01	10	$6.249\,892\,56 \times 10^{-6}$	$3.124\,333\,7792 \times 10^{-5}$
DMRG	5 000	0.002	10	$2.498(36) \times 10^{-7}$	$1.2427(28) \times 10^{-6}$
DMRG	10 000	0.001	10	$6.2(45) \times 10^{-8}$	$3.051(90) \times 10^{-7}$
DMRG	20 000	0.0005	10	$1.(56) \times 10^{-8}$	$7.0(80) \times 10^{-8}$
DMRG	20 000	0.001	20	$6.2(64) \times 10^{-8}$	$3.12(50) \times 10^{-7}$
DMRG	50 000	0.0002	10	$(2.87) \times 10^{-9}$	$(4.99) \times 10^{-9}$
DMRG	50 000	0.0004	20	$(0.961) \times 10^{-8}$	$(5.00) \times 10^{-8}$
DMRG	100 000	0.0001	10	$(-0.71) \times 10^{-8}$	$(-4.15) \times 10^{-8}$
DMRG	100 000	0.0002	20	$(0.16) \times 10^{-8}$	$1(.24) \times 10^{-8}$

are at the middle of the chain. The error bars in the table are given by the amount of variation in the energy during the last finite-system sweep, i.e. the value given is obtained in the last diagonalization step, but the digits in parentheses vary during previous diagonalizations in the sweep. We call this method of estimating the error the global convergence criterium (GCC). However, the GCC is overly restrictive, as can be seen by examining the difference between the continuum ground state energy and the DMRG ground state energy, plotted in figure 3 as a function of the DMRG step during five finite-system sweeps for $N = 3000$ and $h = 0.01$. One can clearly see regions in which the solution has been stabilized as well as depleted regions

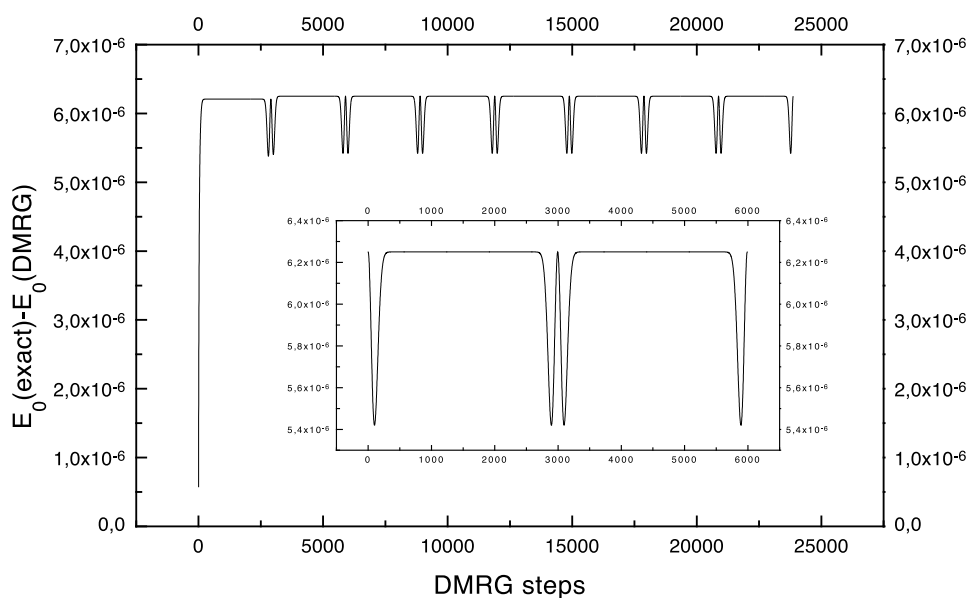


Figure 3. The difference between the ground state energy of the harmonic oscillator obtained with the DMRG during five sweeps for $N = 3000$ and $h = 0.01$, and the exact continuum value. The data plotted starts after convergence in finite-system sweeps has been achieved.

near the ends of the chains in which the DMRG energy is higher. In the inset, we plot the error in energy for a single back-and-forth sweep on an expanded scale. This suggests that the appropriate region to measure the energy must be located away from the ends. We refer to this as a local convergence criterium (LCC). If we adopt the LCC, then the number of stabilized digits increases. This is something which we will examine when comparing DMRG results and exact results in the forthcoming tables.

In figure 3, the DMRG ground state energy converges variationally from above to the exact ground state energy (note that $E_0(\text{DMRG})$ is negated in the plot) for a particular discretization of the system. This energy is close to the plateaus in figure 3 and is lower than the exact continuum energy, i.e. there is a discretization (or finite-size) correction which is not necessarily variational, and which is negative here. This can also be seen in table 1 for the exact diagonalization as well as for the DMRG results.

In table 1 we present several runs in which the final size R of the continuum system is varied in order to check that a convergence has been achieved to a certain number of digits. If R is large enough, the effect of changing it is not very large due to the exponential fall-off of the wavefunctions. We find similar dependence of the error on R for higher excited states. Thus we find that the exact spectrum is very well reproduced by the continuum limit of the DMRG.

In table 1 we also show, when possible, energies obtained via exact diagonalization of the Hamiltonian matrix, equation (1). This is possible for system sizes of up to about $N = 2000$. Exact diagonalization is much more expensive in computer time than DMRG, and yields energies for a particular system size that agree with the DMRG to 14 significant digits. This level of agreement is quite remarkable given that the largest matrix diagonalized in the DMRG procedure is 6×6 .

Table 2. DMRG results for the anharmonic oscillator $H = P^2 + X^2 + CX^4$ in the continuum limit. The notation is the same as that in table 1.

Method	N	h	$R = N \times h$	E_0	E_1	C
DMRG	30 000	0.001	30	1.065 285 43(310)	3.306 871 58(195)	0.1
DMRG	20 000	0.001	20	1.065 285 43(289)	3.306 871 58(195)	0.1
Borel–Padé [8]				1.065 285 50(954)		0.1
Hill [7]				1.065 285 50(954)		0.1
DMRG	30 000	0.001	30	1.392 351 48(046)	4.648 811 63(809)	1
DMRG	20 000	0.001	20	1.392 351 48(038)	4.648 811 63(809)	1
Borel–Padé [8]				1.392 350(6)		1
Hill [7]				1.392 531 6		1
DMRG	30 000	0.001	30	2.449 173(484)	8.598 999 3(093)	10
DMRG	20 000	0.001	20	2.449 173(484)	8.598 999 3(093)	10
Variational [9]				2.449 174 072		10
Borel–Padé [8]				2.440(527)		10
Hill [7]				2.449 174 0		10

6. The anharmonic oscillator

Now that we have checked that the continuum limit of the DMRG accurately reproduces a well known solvable case, we apply DMRG to the anharmonic oscillator, which has no closed analytical solution (see [6] and references therein). Here our purpose is to compare the efficiency of DMRG with that of other standard methods employed in single-particle QM. We treat the Hamiltonian

$$H = P^2 + X^2 + CX^4 \quad (14)$$

where C is a positive coupling constant and we have normalized the mass term.

In table 2, we display the DMRG results obtained using a similar analysis as for the harmonic oscillator. We compute the two lowest energy states, compare them with exact diagonalization results, and obtain the same accuracy as for the harmonic oscillator. We also compare with the results of a number of methods commonly used in standard QM such as the Hill determinant method [7], Borel–Padé approximants of the perturbation series [8] and variational computations in the energy basis of the harmonic oscillator [9].

We have computed the state energies for various coupling constants $C = 0.1, 1, 10$, ranging from weak to strong coupling. We notice that while the Hill determinant method and the Borel–Padé perform better for weak couplings, the continuum limit of the DMRG performs equally well for the whole range of couplings. This is due to the variational nature of the method.

From table 2, one can see that the agreement of the DMRG with the other methods is excellent.

7. The double-well potential

We hope that it is now clear that the DMRG method is an excellent method to compute the energy spectrum and wavefunctions in quantum mechanical problems. We now apply it to an anharmonic oscillator with a potential in the shape of a double well. This problem is particularly interesting for several reasons. One, as we shall see, is that the system has a tunable gap which can be used to investigate the dependence of the convergence of the DMRG on the size of the gap, and the other is its potential as a new non-perturbative method for quantum field theory

problems. We shall not pursue the latter goal here but will only point out that a number of non-perturbative RG techniques have been established since Wilson's original formulation of the RG [10]. These formulations are called exact renormalization group (ERG) because they are based in exact RG flow equations (see [11] for a recent review on this subject). However, since these exact equations are not exactly solvable in general, one usually has to resort to approximate methods in practical applications. The question then arises as to how good these approximations are. In order to check their validity, they are applied to well known problems in single-particle QM. The rationale is that if they are not even able to quantitatively reproduce the physics of these simple systems, their application to truly field theoretical problems would be even less successful.

The Hamiltonian for this potential reads

$$H = P^2 - X^2 + CX^4 \quad (15)$$

where C is the coupling constant and we have normalized the negative mass term. The potential has two minima at the positions

$$x_0^{(\pm)} = \pm \frac{1}{\sqrt{2C}}. \quad (16)$$

Classically, these minima are degenerate in energy. If treated perturbatively, quantum fluctuations can modify the classical energy but not lift the degeneracy. Splitting of the energy levels can only occur if quantum tunnelling between the two wells is taken into account.

In this symmetric potential, the energies can be arranged into pairs $E_n^{(\pm)}$ depending on their even (+) or odd (−) parity. The energy gap from the ground state to the first excited state is then defined as

$$\Delta_0(C) = E_0^{(-)}(C) - E_0^{(+)}(C). \quad (17)$$

In the weak-coupling limit (C very small), the gap $\Delta_0(C)$ can be computed using an instanton approximation plus higher corrections [12], giving the asymptotic formula

$$\Delta_0(C) = 8\sqrt{\frac{\sqrt{2}}{\pi C}} e^{-\frac{\sqrt{2}}{3C}} \left[1 - \frac{71}{1!} \left(\frac{2\sqrt{2}}{12}\right) C - \frac{6299}{2!} \left(\frac{2\sqrt{2}}{12}\right)^2 C^2 - \frac{2691107}{3!} \left(\frac{2\sqrt{2}}{12}\right)^3 C^3 + O(C^4) \right]. \quad (18)$$

This exponentially decreasing behaviour produces an essential singularity in the energy gap. Our purpose is to capture this highly nontrivial behaviour with the DMRG.

One can understand what happens to the system in the weak coupling limit on physical grounds. From equation (16), we see that the distance between the minima diverges as $C \rightarrow 0$, so that we effectively end up with a system formed by two independent potential wells. The system then becomes exponentially degenerate for each pair of energy levels and thus gapless.

It is also interesting to use this quantum mechanical example to test the behaviour of DMRG for gapless systems. This is a very important issue when dealing with the strongly interacting quantum many-body systems to which DMRG is usually applied. Since its early development, it has been known that the the DMRG method [1] produces much more accurate results for finite correlated systems with a gap than for gapless systems. For gapless systems one has to use the finite-system algorithm on larger system sizes than for gapful systems in order to obtain results of comparable accuracy [13]. We show below that the DMRG handles well the case in which the gap between the ground state and the first excited state becomes negligibly small, i.e. when the two minima of double-well potential are far apart.

Table 3. DMRG results for the double-well potential $H = P^2 - X^2 + CX^4$ in the continuum limit. The notation is the same as that in table 1. R–R stands for the results obtained with the Rayleigh–Ritz method explained in the text.

Method	C	N	h	E_0	Δ
DMRG	1	1 000	0.01	0.657 644 253 61(29)	2.176 825 710(298)
Exact diag.	1	1 000	0.01	0.657 644 253 611 7	2.176 825 710 302
DMRG	1	20 000	0.0005	0.657 652 983(568)	2.176 883 05(297)
R–R	1			0.657 653 005 181	2.176 883 197 05
DMRG	0.6	20 000	0.0005	0.391 952 61(873)	1.633 284 7(928)
R–R	0.6			0.391 952 633 37	1.633 284 884 6
DMRG	0.1	40 000	0.001	−1.265 492 92(138)	0.112 433 68(739)
R–R	0.1			−1.265 492 837 21	0.112 433 706 14
Inst.	0.1				0.114 474 508 49
DMRG	0.06	60 000	0.0005	−2.823 639 49(203)	0.007 299 766 1(673)
R–R	0.06			−2.823 639 458 45	0.007 299 752 6870
Inst.	0.06				0.007 313 907 0463
DMRG	0.02	90 000	0.0004	−11.106 472 434(074)	$2.1(074) \times 10^{-9}$
R–R	0.02			−11.106 472 414 954	$2.104 3 \times 10^{-9}$
Inst.	0.02				$2.107 37 \times 10^{-9}$

In table 3, we present the results for the lowest two energy levels and the gap upon varying the coupling constant from $C = 1.0$ – 0.1 . These values range from the strong- to the weak-coupling regime. The DMRG results are obtained as described previously after five finite-system sweeps. We also compare with exact diagonalization methods when $N < 2000$ and find excellent agreement, typically up to ten digits or better.

In table 3, we have also computed the energy variationally using the Rayleigh–Ritz method [6] (R–R). We compute the expectation value of the Hamiltonian, equation (15), in the energy basis of the harmonic oscillator consisting of up to $M = 1000$ states. In this representation, the non-vanishing elements of the Hamiltonian lie within a band and are given by

$$\begin{aligned}
 \langle n|H|n\rangle &= C\left[\frac{1}{4}n(n-1) + \frac{1}{4}(2n+1)^2 + \frac{1}{4}(n+1)(n+2)\right] \\
 \langle n|H|n+2\rangle &= -\sqrt{(n+2)(n+1)} + C\left[\sqrt{(n+1)(n+2)}\left(n + \frac{3}{2}\right)\right] \\
 \langle n|H|n+4\rangle &= C\frac{1}{4}\sqrt{(n+4)(n+3)(n+2)(n+1)}.
 \end{aligned} \tag{19}$$

In this representation, the Hamiltonian is already in the continuum limit. The R–R theorem states that the M resulting energy levels will be upper bounds to the first M exact energy levels. As seen in figure 4, the agreement between exact and DMRG methods is excellent for this range of the coupling constant and, in fact, the curves appear overlapped in the plot.

Recently, one ERG method was applied to the study of the double-well potential with the aim of probing the method in the whole range of coupling constants [14]. This method is based on the solution of the local potential approximation of the Wegner–Houghton equation [15, 16]. The outcome of these investigations is that the ERG performs very well in the strong-coupling regime where no perturbation treatment is available. However, in the weak-coupling limit, the ERG fails to reproduce the behaviour found with the instanton formula, equation (18).

To check the performance of the DMRG as compared with the instanton formula, equation (18), in the very weak-coupling limit, we have extended our computations from $C = 0.1$ – 0.02 , where the gap becomes as small $\mathcal{O}(10^{-9})$. In table 3 and in figure 4, we present the results from the DMRG, R–R and the instanton formula. We see that DMRG is an excellent non-perturbative method in the entire range of coupling constants and that it is able to quantitatively capture the exponentially decreasing behaviour of the gap.

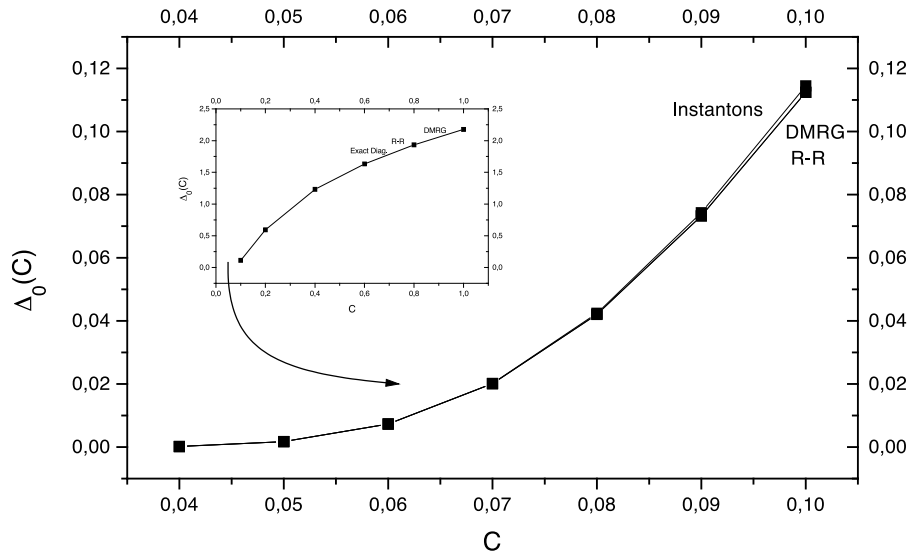


Figure 4. Energy gap $\Delta_0(C)$ in the anharmonic double-well potential as a function of the coupling constant C in the very weak coupling regime (table 3). Here the results of the three methods: the DMRG, instanton calculation and R-R overlap. Results for a wider range of C (table 3) are shown in the inset.

8. Conclusions and prospects

The DMRG method we have presented in this paper is a natural extension of one introduced by White to illustrate the DMRG algorithm for the most simple problem: a free particle on a tight-binding chain [3]. We have shown that the DMRG works with very high precision, yielding an accurate determination of the lowest energy levels for three different potentials: the harmonic oscillator, the anharmonic oscillator and the double-well potential. Its performance is better than or comparable with other known perturbative and non-perturbative methods. For single-particle QM, the DMRG does not require the use of a density matrix. The number of states retained in the RG procedure is equal to the number of states to be obtained, N_E . Aside from N_E , the variational wavefunction of the DMRG has no adjustable parameters.

Single-particle QM has been widely used in the past as a testing ground for concepts or techniques that can be applied to more complex systems. With this in mind, we have studied quantum tunnelling through a potential barrier for the double-well potential and found a value of the gap very close to the exact one for a large range of coupling constants. This is an interesting result because it shows that the DMRG can, in principle, handle tunnelling phenomena better than other methods such as the ERG [14]. An interesting topic for future work would be to explore to what extent this feature holds for many-body systems or for field theory.

Although the DMRG was originally developed as a ground state technique, there have recently been new developments in using it to obtain dynamical information [17, 18]. In the context of single-particle QM, one could ask whether the DMRG could give information about phase shifts, decay rates, etc. These and other questions remain to be investigated.

Acknowledgments

We would like to thank A Galindo and S R White for useful conversations on this topic.

We would like to thank the Max Planck Institute for the Physics of Complex Systems in Dresden for support to participate in the DMRG98 Seminar/Workshop, at which this work was initiated.

MAMD and GS acknowledge support from the DIGICYT under contract No PB96/0906, and RMN acknowledges support from the Swiss National Foundation under grant nos 20-46918.96 and 20-53800.98.

References

- [1] White S R 1992 *Phys. Rev. Lett.* **69** 2863
White S R 1993 *Phys. Rev. B* **48** 10 345
- [2] White S R and Noack R M 1992 *Phys. Rev. Lett.* **68** 3487
- [3] White S R 1998 *Phys. Rep.* **301** 187
- [4] Noack R M and White S R 1999 *The Density Matrix Renormalization Group (Lecture Notes in Physics)* ed I Peschel, X Wang and K Hallberg (Berlin: Springer) ch 3
- [5] Legeza Ö and FÁth G 1998 *Preprint cond-mat/9809035*
- [6] Galindo A and Pascual P 1990 *Quantum Mechanics (Text Monographs in Physics)* vol II (Berlin: Springer)
- [7] Biswas S N, Datta K, Saxena R P, Srivastava P K and Varma V S 1971 *Phys. Rev. D* **4** 3617
- [8] Graffi S et al 1970 *Phys. Lett. B* **32** 631
- [9] Balsa R, Plo M, Esteve J G and Pacheco A F 1983 *Phys. Rev. D* **28** 1945
- [10] Wilson K G and Kogut J B 1974 *Phys. Rep.* **12** 75
- [11] 1998 *Proc. Workshop on the Exact Renormalization Group (Faro, Portugal, September 10–12)* (Singapore: World Scientific)
- [12] Seznec R and Zinn-Justin J 1979 *J. Math. Phys.* **20** 1398
- [13] Andersson M, Boman M and Ostlund S 1999 *Phys. Rev. B* **59** 10 493
(Andersson M, Boman M and Ostlund S 1998 *Preprint cond-mat/9810093*)
- [14] Aoki K-I, Horikoshi A, Taniguchi M and Terao H 1998 *Preprint hep-th/9812050*
- [15] Wegner F and Houghton A 1973 *Phys. Rev. A* **8** 401
- [16] Aoki K-I, Morikawa K, Souma W, Sumi J-I and Terao H 1998 *Prog. Theor. Phys.* **99** 401
- [17] Hallberg K A 1995 *Phys. Rev. B* **52** 9827
- [18] Kühner T D and White S R 1999 *Phys. Rev. B* **60** 335
(Kühner T D and White S R 1998 *Preprint cond-mat/9812372*)